Indonesian Journal of Maritime Technology (ISMATECH)
Vol. 3, Issue 2, December 2025
eISSN: 3025-518X
DOI: https://doi.org/10.35718/ismatech.v3i2.8481434

Comparison of Motion Response Characteristics of Tension Leg Platform Structure Threestar and Fourstar

Rafi Irsyad Syarief[1], Luh Putri Adnyani[1]*, Destyariani Liana Putri[1]

[1]Department of Ocean Engineering, Institut Teknologi Kalimantan, Balikpapan, 76127, Indonesia

KEYWORDS
Tension Leg Platform
Pontoon Configuration
Motion Response
Free Floating
Six Degree of Freedom

ABSTRACT – Tension Leg Platform (TLP) is a floating structure used for deep-sea oil and gas exploration with a tendon mooring system that maintains its stability. This study aims to compare the dynamic response of two TLP configurations, namely Threestar and Fourstar, during free-floating. Modeling is conducted numerically using ANSYS SpaceClaim and hydrodynamic simulation through ANSYS AQWA. The structural dimensions are modified from TLP A West Seno using displacement as validation. Environmental loading is based on wave, wind, and current data from the Makassar Strait waters. The simulation results show that the Threestar configuration has a higher Response Amplitude Operator (RAO) value in translational and rotational movements than Fourstar, except for heave movements where Fourstar is slightly more dominant. The difference in RAO values reflects the effect of the number and configuration of pontoons on structural stability. Fourstar, which is more symmetrical to the X and Y axes, shows a more stable response. In addition, TLP structures tend to show better performance in longer wave periods. Thus, the Fourstar structure is more recommended as it provides higher stability in challenging sea conditions.

*Corresponding Author | Luh Putri Adnyani | ✉ luhputria@lecturer.itk.ac.id

INTRODUCTION

Tension leg platform (TLP) is one type of offshore structure specifically designed for deepwater oil and gas exploration and production. TLP uses tendons embedded in the seabed, which keep the platform stable above the water surface by reducing vertical movement (heave) and providing resistance to extreme marine environmental conditions [1]. However, TLP operations face significant challenges, especially in understanding and predicting the dynamic response of the structure to various environmental conditions such as waves, wind, and ocean currents. The dynamic response of TLP is highly dependent on the configuration of the structure design and the type of mooring used to maintain stability. In this case, the type of mooring used is a tendon (tether) where the TLP is moored by tendons so that this structure is safer until it only experiences one degree of freedom, namely surge [2, 3]. This study investigates motion characteristics of TLP, especially column and pontoon, excluding the topside investigation that can be found in Rosyid and Djatmiko [4].

The difference in pontoon configuration in facing environmental loads, that TLP with circular pontoons provides a more stable dynamic response and is less affected by the angle of incoming waves compared to square pontoons [5]. The rise in sea level affects the increase in structural response due to the cross-section immersed in wider water [6]. Heading or environmental load direction also affects the motion of a floating structure [7].

Previous researchers investigated TLP using numerical and physical modelling [8] and parametric approach [9]. A series of small-scale wave tank tests on four column TLP models is focused on interaction phenomena such as wave run-up on the vertical legs and the amplification of the waves beneath the deck [1]. Different wave conditions impact the platform, including a first-order irregular wave, a second-order wave, and a freak wave impact against the platform are investigated by Wang, et al. [10]. The recent studies are more focused on using TLP as floating offshore wind turbines (FOWT) [11]. Chang, et al. [12] investigated the dynamic responses of a TLP in a freak wave, considering the influences of second-order wave forces.

Therefore, it is necessary to observe the dynamic response of the TLP structure with a combination of three-star and four-star pontoons under a free-floating scenario. This study is related to Xu, et al. [13] that conducted a comparative study on the dynamic responses under environmental loading conditions by altering the tension legs' connection angle. The purpose of this study is to determine the comparison of the dynamic response of the three-star and four-star TLP structures in free-floating conditions. The desired result in this study is a TLP design that has optimal structural motion in free-floating conditions.

METHODS

Tension Leg Platform Structure Dimension

The structural dimension data used refers to the TLP A West Seno structure, then applied to the Mono-column three-star and four-star structures. The main dimensions of the TLP A West Seno structure are in Table 1, and the main dimensions of the TLP three-star and four-star structures are in Table 2.

Table 1. Main Dimension TLP A West Seno [4]

Item		**TLP A West Seno**
Column	Shape	Square
	Geometry	9.6 m x 9.6 m x 36.26 m
	Qty	4
Pontoon	Shape	Square
	Geometry	9.6 m x 9.6 m x 32.1 m
	Qty	4
Design Draft		28,95 m
Displacement		23059 MT

Table 2. Threestar and Fourstar TLP Dimension [4, 14]

Item		**Design**	
		Threestar	Fourstar
Column	Shape	Cylindrical	Cylindrical
	Dimension	r = 9 m x L = 38,1 m	r = 9 m x L = 38,1 m
	Qty	1	1
Pontoon	Shape	Square	Square
	Dimension	10 m x 10 m x 50,9 m	10 m x 10 m x 50,9 m
	Qty	3	4
Draft		28,95 m	28,95 m

Tension Leg Platform Structure Dimension

The TLP structure is modeled using Ansys SpaceClaim software. The result of design model is shown in Figure 1.

Model Validation

To find out whether the modelled TLP structure has a displacement that is close to the displacement of the TLP A West Seno structure, the error value between the modelled structure and the reference structure must be considered. Based on DNV GL Rules for Ships, the error value for validating the displacement model design is 2% [15]. Table 3 gives the error value between the modelled structure and the reference structure

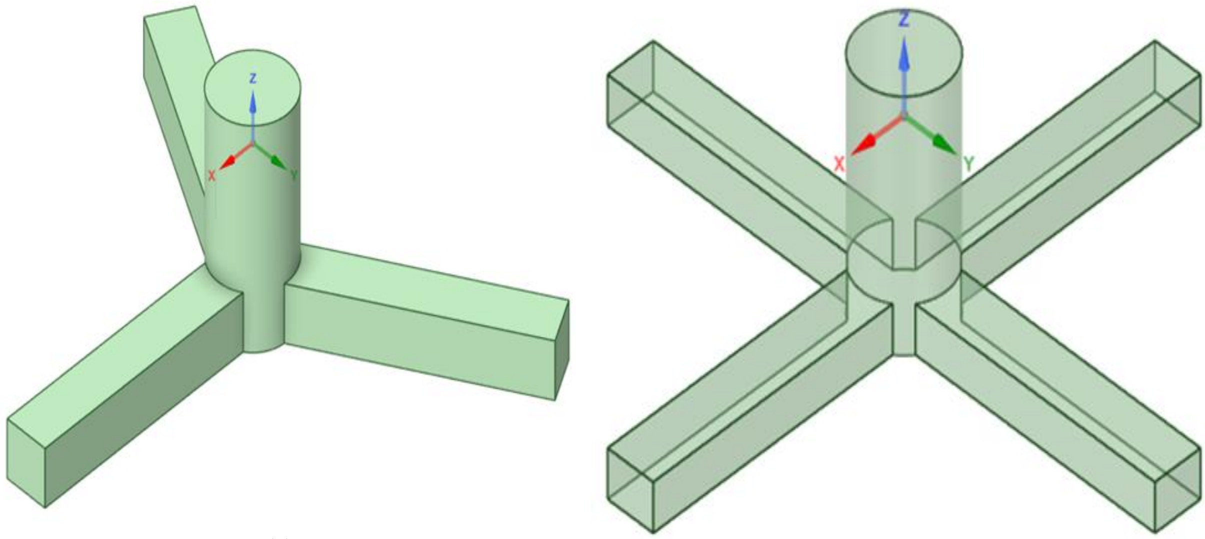

(a) (b)

Figure 1. Model Design (a) Threestar (b) Fourstar

Table 3. Displacement Validation

Structure	Unit	Model displacement	Existing displacement	Error
Threestar	Ton	22620,623	22602	0,08%
Fourstar	Ton	22668,089	22602	1,70%

Environmental Data

Load modelling using environmental data at the West Seno Field located in the Makassar Strait waters.

Table 4. West Seno Field Environmental Data

Parameter	Value	
	1 years	100 years
H max (m)	3,26	4,97
T max (sec)	7,6	8,1
Wind Speed (m/s)	9,25	13,99
Surface Current (m/s)	0,41	0,54
Tidal Range (m)	2,50	2,50
Storm Surge (m)	0	0,49

RESULTS AND DISCUSSION

This study analyses how the motion characteristics occur when the TLP three-star and four-star are floating freely. From the analysis carried out, the RAO of the three-star structure will be compared with that of the four-star structure. This analysis uses Ansys AQWA software. Figures below show RAO under five headings: flow, from the 0° direction to represent following seas, the 90° direction to represent beam seas and the 45° direction to represent quartering seas.

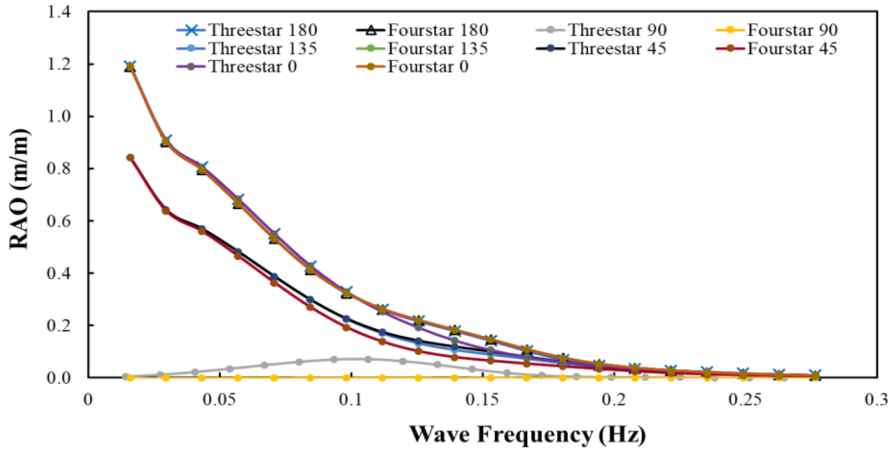

Figure 2. Surge RAO Motion of Threestar and Fourstar

As shown in Figure 2, the RAO amplitude demonstrates a clear inverse relationship with wave frequency, consistent with theoretical expectations for low-frequency dominant surge responses in floating systems. At low wave frequencies (0.03–0.05 Hz), both configurations exhibit peak RAO values, indicating resonant-like behavior where the wave-induced surge motion is amplified due to the low hydrodynamic damping. In particular, Fourstar 0° and Threestar 0° attain the highest RAO magnitudes, reaching values of approximately 1.2 m/m and 1.15 m/m, respectively. This suggests that waves approaching directly along the longitudinal axis of the multibody system (0° heading) induce the largest surge displacements. The symmetrical alignment allows for maximum energy transfer in the surge direction.

As the wave heading increases toward the beam sea direction (90°), there is a notable reduction in surge RAO, especially for the Fourstar 90° case, which approaches near-zero values across all frequencies. This outcome aligns with the physical expectation that waves striking perpendicular to the main axis of the structure excite sway and roll rather than surge motion. Across the frequency range, the Fourstar configuration generally exhibits slightly higher RAO values compared to the Threestar configuration at head and following seas (0°, 180°). This is likely attributed to its larger projected frontal area and more complex hydrodynamic interaction due to the additional unit. However, at beam seas, both configurations show significantly suppressed surge responses, which confirms the directional sensitivity of multibody systems in free-floating conditions. Furthermore, all configurations show a steep decay in RAO magnitude beyond 0.1 Hz, indicative of the inertial dominance and radiation damping that become significant at higher wave frequencies. The trend across all headings highlights that surge motion is primarily governed by low-frequency wave excitation, which is a critical consideration for mooring design, offloading operations, and dynamic positioning systems. It can be seen that for the surge movement, the highest motion value is from the following sea direction parallel to the x-axis, which occurs because the surge movement translates on the x-axis.

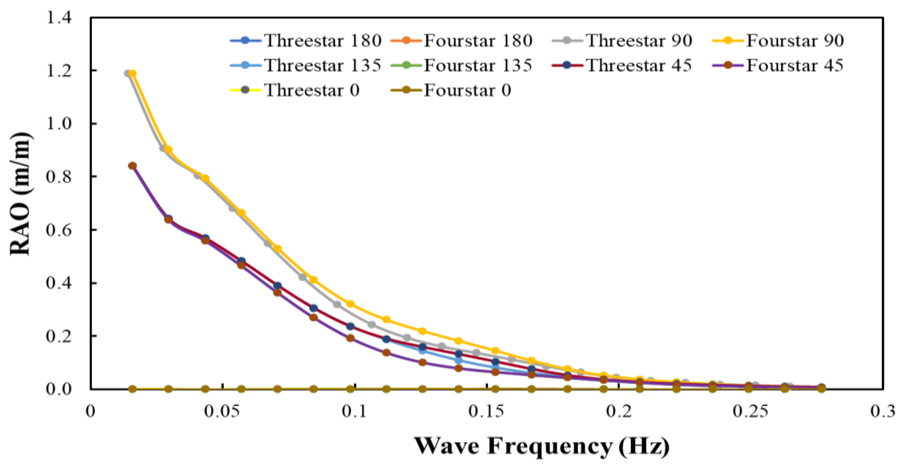

Figure 3. Sway RAO Motion of Threestar and Fourstar

Figure 3 presents RAOs in sway motion for Threestar and Fourstar, subjected to incident wave directions of 0°, 45°, 90°, 135°, and 180°. The RAO values (in m/m) are plotted against a range of wave frequencies (Hz), allowing comparison of the hydrodynamic response characteristics under varying directional wave conditions. Overall, the RAO amplitudes decrease with increasing wave frequency for all configurations and headings, which is consistent with typical floating structure behavior. At low frequencies (around 0.02–0.05 Hz), the Fourstar 90° condition exhibits the highest RAO value, reaching approximately 1.2 m/m, indicating greater sensitivity to long-period waves from beam directions. In contrast, the Fourstar 0° configuration shows a negligible response across all frequencies, suggesting strong directional stiffness or damping in head-sea conditions. Similarly, Threestar 0° displays slightly higher responses than Fourstar 0° but remains among the lowest. Comparing both configurations, Fourstar generally yields higher RAOs than Threestar, particularly at low frequencies and for beam (90°) and oblique wave incidences (135°, 180°), implying a greater wave-induced motion under such directions. This could be attributed to differences in mooring line arrangements or platform geometry.

These results highlight the critical influence of wave direction and mooring layout on the heave response of the floating structure and demonstrate the importance of directional RAO assessment in preliminary design and stability evaluation. Some movements have different graphic shapes, indicating that the configuration of the number of pontoons affects the TLP motion. The highest value in the sway movement is from the beam sea direction parallel to the y-axis, because the sway movement translates on the y-axis.

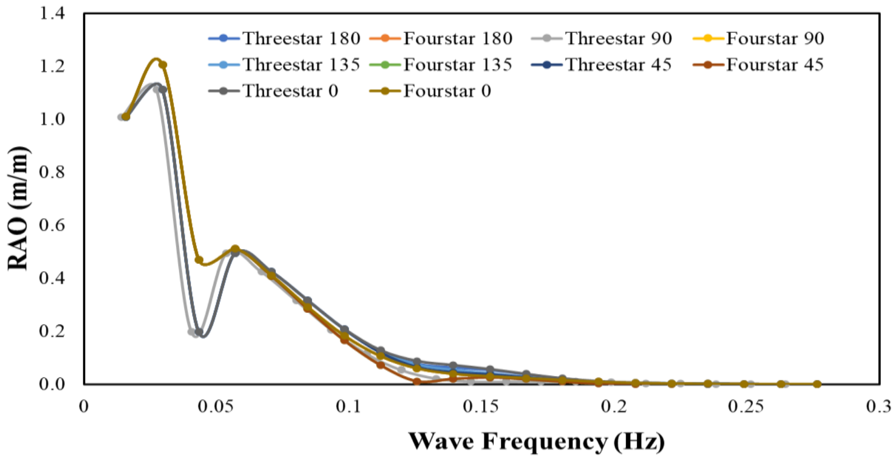

Figure 4. Heave RAO Motion of Threestar and Fourstar

Figure 4 illustrates the heave RAOs as a function of wave frequency (Hz) for Threestar and Fourstar—under multiple wave incidence directions (0°, 45°, 90°, 135°, and 180°). The RAO is expressed in meters per meter (m/m), representing the amplitude ratio between platform heave motion and incoming wave amplitude. A prominent peak is observed around 0.035 Hz to 0.04 Hz for all configurations, indicating a resonant frequency in the heave response. Among the cases, the Fourstar 90° configuration exhibits the highest RAO value, exceeding 1.2 m/m, followed by comparable peaks in Threestar 90° and Fourstar 180°, suggesting that the structure is more susceptible to vertical excitation when waves approach from beam and stern directions. In contrast, both Threestar 0° and Fourstar 0° display lower peak responses, although Fourstar 0° shows a slightly elevated RAO, indicating that the Fourstar layout may have reduced directional stiffness along the longitudinal axis.

Beyond the resonance frequency, all RAO curves show a rapid decay with increasing wave frequency, consistent with the dynamic response of compliant floating structures in deep water. The decay becomes nearly asymptotic after 0.2 Hz, indicating minimal dynamic amplification at higher frequencies. The second minor peak observed around 0.06 Hz could be attributed to secondary resonance modes or interaction effects between mooring stiffness and hydrodynamic forces. The comparison between Threestar and Fourstar configurations across all headings suggests that Fourstar arrangements tend to produce slightly higher RAOs at resonance but follow similar attenuation trends at higher frequencies. This indicates that while both mooring layouts maintain overall hydrodynamic stability, Fourstar may experience more pronounced motions under long-period wave conditions. For the heave movement, from the following seas and beam seas directions have the same graphic trend because the heave movement translates on the z-axis or vertical.

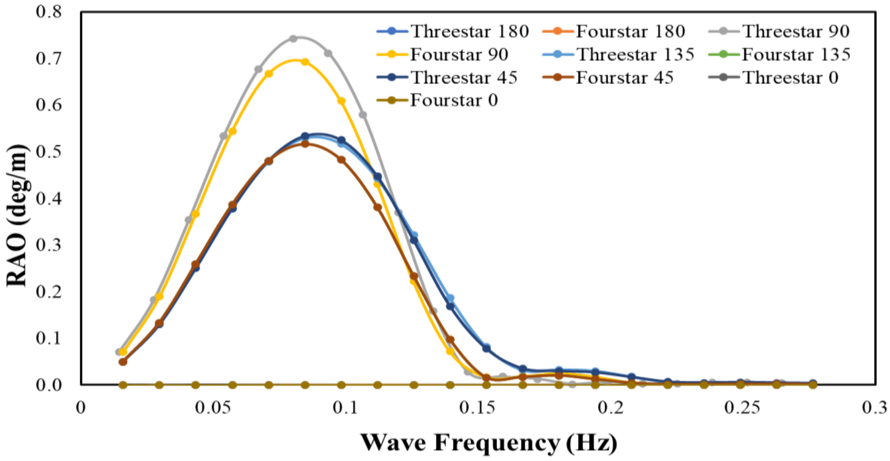

Figure 5. Roll RAO Motion of Threestar and Fourstar

Figure 5 illustrates the roll RAOs, expressed in degrees per meter (deg/m), representing the angular roll response per unit wave amplitude. The wave frequency ranges from 0 to 0.3 Hz, encompassing the primary dynamic range of interest for offshore floating systems. A clear resonance peak is observed across most configurations within the frequency band of 0.06–0.09 Hz, indicating the natural frequency of roll motion for the moored system. The Threestar 90° configuration demonstrates the highest peak RAO, reaching approximately 0.73 deg/m, followed closely by the Fourstar 90°, suggesting that both mooring layouts are particularly sensitive to beam wave excitations. This behavior aligns with the expected roll amplification due to transverse wave loading on the structure.

In contrast, Fourstar 0° yields negligible roll response across all frequencies, reflecting strong directional stiffness or damping in head-sea conditions. Similar behavior is also observed for Threestar 0°, indicating that both configurations effectively suppress roll motion when waves propagate longitudinally along the hull. Notably, the RAO curves of Fourstar 180° and Threestar 180° remain relatively moderate, implying a balanced roll response to stern-sea conditions. Meanwhile, intermediate directions (45°, 135°) show smooth and symmetric resonance profiles with moderate amplitudes (peaking between 0.45–0.55 deg/m), indicating that oblique wave incidence leads to less critical roll resonance compared to beam seas.

Beyond the resonant peak, all configurations exhibit a sharp decline in RAO magnitude with increasing wave frequency, becoming asymptotically low beyond 0.15 Hz. This trend reflects the natural damping behavior of the system, where high-frequency waves are insufficient to excite significant roll motion due to inertial constraints and hydrodynamic damping. These findings highlight the importance of wave directionality and mooring configuration in governing the roll motion performance of floating platforms. While the Fourstar system offers comparable roll mitigation performance to Threestar, the latter may pose increased susceptibility to transverse wave loads, especially around the resonant range. The largest roll movement comes from the direction of the beam sea because in the beam sea the waves are perpendicular to the TLP.

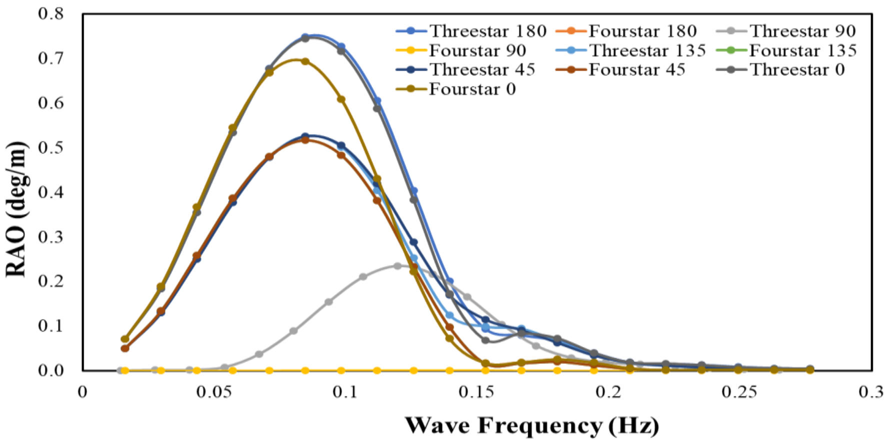

Figure 6. Pitch RAO Motion of Threestar and Fourstar

Figure 6 presents the roll RAOs. A distinct resonance behavior is observed in the frequency range of 0.07–0.1 Hz, where the majority of configurations exhibit peak roll motion. The Threestar 180° and Fourstar 0° cases record the highest RAO values, peaking at approximately 0.73 deg/m, suggesting that these configurations are most susceptible to roll excitation under stern and head-sea wave directions, respectively. This indicates that both configurations are less directionally stable under longitudinal wave forcing. In contrast, the Fourstar 90° and Threestar 90° configurations exhibit minimal response across all frequencies, with Fourstar 90° remaining effectively unresponsive throughout the spectrum. This indicates significant damping or stiffness in the beam-sea direction for the Fourstar layout, providing enhanced roll mitigation.

For quartering sea (45° and 135°), both configurations demonstrate moderate resonance amplitudes (around 0.5–0.55 deg/m), with consistent trends suggesting symmetric roll responses for oblique wave headings. Notably, Threestar 135° and Fourstar 135° show slightly broader response curves compared to the sharper peaks in head- and following-sea directions, which may reflect modal coupling or mooring-induced asymmetry in restoring moments. As wave frequency increases beyond resonance (>0.15 Hz), all RAO curves exhibit a rapid decline, converging to near-zero response, which reflects the reduced efficiency of high-frequency waves in exciting roll motion due to inertial resistance and added hydrodynamic damping.

Overall, the results indicate that while Fourstar mooring shows superior roll suppression in beam directions, it is more sensitive in head-sea conditions. Conversely, Threestar exhibits relatively balanced behavior across headings but shows higher peaks under stern-sea excitation. These findings are critical for assessing platform stability and fatigue design, particularly for floating systems deployed in multi-directional wave environments. The pitch movement is influenced by the head sea, which occurs because the pitch rotates on the y-axis or laterally, which is parallel to the head sea.

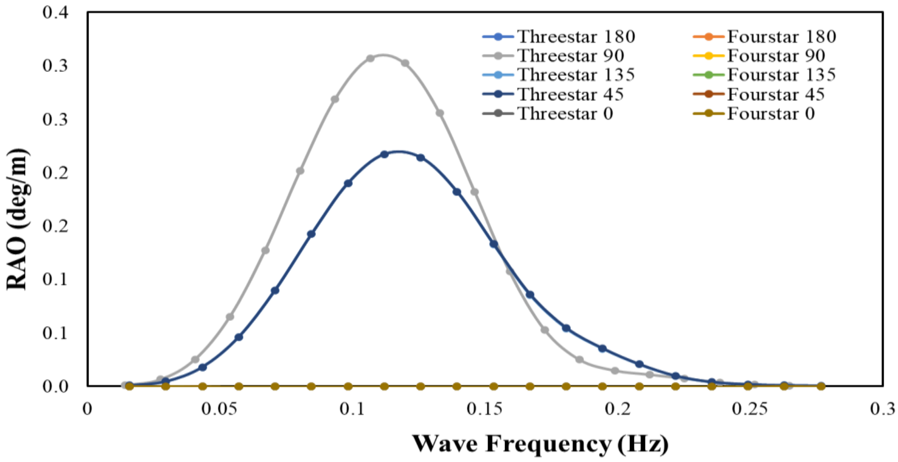

Figure 7. Yaw RAO Motion of Threestar and Fourstar

Figure 7 presents the yaw RAOs. Among the configurations, only Threestar display significant yaw motion. In particular, the Threestar 90° case exhibits the highest peak RAO, reaching approximately 0.32 deg/m at a frequency of around 0.1 Hz, corresponding to the natural yaw resonance of the system under beam wave conditions. Similarly, Threestar 45° and Threestar 180° show notable responses, with peak values near 0.22 deg/m, indicating the directional dependence of yaw excitation. In contrast, all Fourstar configurations exhibit negligible yaw response across the entire frequency range, remaining flat and near zero. This suggests that the Fourstar mooring layout effectively suppresses yaw motion, possibly due to increased symmetry or higher restoring moments in the yaw degree of freedom.

The yaw response in the Threestar system decreases steadily at higher frequencies (>0.15 Hz), indicating that wave components beyond this range do not significantly excite rotational motion. The discrepancy in yaw sensitivity between configurations highlights the importance of mooring arrangement and wave incidence direction in determining platform heading stability. These results underscore the superior yaw damping performance of the Fourstar configuration and the potential vulnerability of the Threestar layout to beam wave-induced yaw, which may be critical for station-keeping and heading control in operational conditions. The highest RAO is when heading from the direction of the beam sea because the environmental load is considered to hit from the side, so that rotation occurs on the z-axis.

In general, the surge motion caused by the beam seas direction, and the threestar structure experiences a higher motion than the four-star structure, which occurs because the pontoon configuration in the threestar structure is asymmetrical to the x and y axes. The maximum motion response value in the threestar structure is 0.716 m/m under operating conditions, 0.718 m/m under extreme conditions, while for the fourstar structure it is 0.000453 m/m under operating conditions, 0.00045 m/m under extreme conditions. Similar to the sway translational motion, in the rotational motion of roll, pitch and yaw, the threestar structure has a greater response than the fourstar structure. The threestar structure, which has a 120o configuration tends to have a greater rotational motion response than the fourstar structure which has a more symmetrical configuration, namely 90o between pontoon. However, in the heave translational motion, the fourstar structure has a slightly greater response value than the fourstar structure. This happens because the number of pontoons in the four-star structure is 4 structures compared to the threestar structure, which only has 3 items. These findings emphasise the importance of wave directionality and tendon design in optimising the motion performance of floating platforms, particularly in environments dominated by long swell or low-frequency sea states.

CONCLUSION

It can be concluded that the variation of the number of pontoons in the TLP structure greatly affects the RAO value of 6 degrees of freedom (6 DOF), namely surge, sway, heave, roll, pitch, and yaw. The four-star structure generally has a lower RAO compared to the three-star structure, which means it is more stable because it is influenced by the configuration of the pontoons, which are symmetrical to the x and y axes. The motion characteristic of TLP, based on the 6 DOF of TLP, depends on the wave heading.

REFERENCES

[1] J. Niedzwecki and J. Huston, "Wave interaction with tension leg platforms," *Ocean Engineering*, vol. 19, no. 1, pp. 21-37, 1992.

[2] S. Chandrasekaran and K. Yuvraj, "Dynamic analysis of a tension leg platform under extreme waves," *Journal of Naval Architecture and Marine Engineering*, vol. 10, no. 1, pp. 59-68, 2013.

[3] L. Purwanti, "Analisa Vortex Induced Vibration Pada Riser Tension Leg Platform," *Jurnal Teknik Kelautan, Institut Teknologi Sepuluh Nopember*, 2008.

[4] S. S. N. D. M. Rosyid and E. B. Djatmiko, "Analisis Kegagalan Ultimate pada Topside Support Structure Seastar Tension Leg Platform (TLP) dengan Metode Incremental Extreme Load."

[5] J. Akmal, "RESPON DINAMIS TENSION LEG PLATFORM (TLP): STUDI KOMPARASI ANTARA PENGGUNAAN PONTON TELAPAK LINGKARAN DENGAN PONTON TELAPAK BUJUR SANGKAR," *Machine: Jurnal Teknik Mesin*, vol. 8, no. 1, pp. 45-50, 2022.

[6] Y. A. Wibowo, R. D. Riyanto, L. Alfaris, and A. Baswantara, "SOLUSI ANALITIK RESPON GERAKAN SURGE OCEAN THERMAL ENERGY CON-VERSION BERBENTUK TENSIONED LEG PLATFORM (OTEC-TLP)," 2022.

[7] L. P. Adnyani and R. G. Harahap, "Karakteristik Respon FPSO Konversi Tanker Ukuran 310 M," *JURNAL SAINTIS*, vol. 19, no. 1, pp. 1-7, 2019.

[8] D. Walia, P. Schünemann, H. Hartmann, F. Adam, and J. Großmann, "Numerical and physical modeling of a tension-leg platform for offshore wind turbines," *Energies*, vol. 14, no. 12, p. 3554, 2021.

[9] E. E. Bachynski and T. Moan, "Design considerations for tension leg platform wind turbines," *Marine Structures*, vol. 29, no. 1, pp. 89-114, 2012/12/01/ 2012, doi: https://doi.org/10.1016/j.marstruc.2012.09.001.

[10] J. Wang, Y. Luo, Y. Wang, R. Guo, W. Cai, and J. Zhao, "Dynamic response of tension leg platform with hydro-pneumatic tensioner under second-order waves and freak waves," *Ocean Engineering*, vol. 252, p. 111261, 2022.

[11] D. Kim, Y. H. Bae, and S. Park, "Design strategy for resonance avoidance to improve the performance of tension leg platform-type floating offshore wind turbines," *Ocean Engineering*, vol. 306, p. 118080, 2024.

[12] S. Chang, W. Huang, F. Liu, and H. Song, "Influence of second-order wave force and focusing position on dynamic responses of tension leg platform under a freak wave," *Ocean Engineering*, vol. 242, p. 110126, 2021.

[13] X. Xu, N. Wei, and W. Yao, "The stability analysis of tension-leg platforms under marine environmental loads via altering the connection angle of tension legs," *Water*, vol. 14, no. 3, p. 283, 2022.

[14] Cendrawani, "Studi Komparasi Perilaku Dinamis Tension Leg Platform Kolom Tunggal Bertelapak Kaki Bintang Tiga dan Bintang Empat dengan Pendekatan Pembebanan Berdasar Teori Morison dan Difraksi," Tugas Akhir Jurusan Teknik Kelautan, Institut Teknologi Sepuluh Nopember, Surabaya, 2012.

[15] *Rules for Classification: Ships, Part 3 Chapter 1 – Hull Structural Design, General, Det Norske Veritas Germanischer Lloyd*, D. GL, [Online], 2020. [Online]. Available: https://rules.dnv.com